ASTRONOMY & ASTROPHYSICS
SUPPLEMENT SERIES

Astron. Astrophys. Supl. Ser. **130**, 267–283 (1998)

Star formation history of early-type galaxies in low density environments⋆

II. Kinematics

M. Longhetti[1], **R. Rampazzo**[1], **A. Bressan**[2], **and C. Chiosi**[3]

[1] Osservatorio Astronomico di Brera, Via Brera 28, I–20121, Milano, Italy
[2] Osservatorio Astronomico di Padova, Vicolo dell'Osservatorio, 5, I-35122 Padova, Italy
[3] Dip. di Astronomia, Univ. di Padova, Vicolo dell'Osservatorio, 5, I-35122 Padova, Italy

Received July 1; accepted September 15, 1997

Abstract. The present paper is a companion of two others dedicated one to the measurement of the line–strength indices (Longhetti et al. 1997a) and the second to trace back the star formation history of a sample of early–type galaxies by comparing observed indices to the predictions of new spectro–photometric models (Longhetti et al. 1997b).

The sample of 51 early-type galaxies in low density environments is composed of two sub-sets of galaxies: 21 shell galaxies from the Malin & Carter (1983) catalogue (one of which shows double nucleous and has been considered as two separate objects) and 30 members of isolated interacting pairs from the Reduzzi & Rampazzo (1995) catalogue. Most of the objects show fine structures.

The paper collects nuclear kinematic data together with the velocity and velocity dispersion curves of the stellar and gaseous components as a function of the distance from the galaxies centres. The galaxies heliocentric systemic velocity compares within -1 ± 32 km s^{-1} with RC3 data, while their central velocity dispersion compares within 9 ± 9 km s^{-1}, 10 ± 27 km s^{-1} and 2 ± 33 km s^{-1} with Gonzalez (1993), Davies et al. (1987) and Carter et al. (1988) respectively. The detailed comparison between our velocity and velocity dispersion curves and those from several authors is discussed.

9 out of 22 shell galaxies nuclei show emission lines, 4 of which, using data in the literature, have line ratios characteristic of LINERs. 10 members of pairs out of 30 show emission lines. RR 331a has a Seyfert like nucleus, while for the remaining galaxies the ([O III] λ 5007)/Hβ ratio is characteristic of low ionization regions. In a small fraction of the objects the emission component is detectable outside the central value. None of the objects in the sample shows counter-rotation of the gaseous versus the stellar component. The two components appear associated, although, in two cases there is evidence that gas and stars lie on different planes. This latter phenomenon could be associated to accretion events. Emission lines in the central part of the RR 331a show a secondary component in the emission lines profile.

E 2400100 has two nuclei embedded in the main body of the galaxy. The U-shape profile of the stellar velocity profile shows the ongoing interaction of the two nuclei. V/σ profile of shell galaxies is, finally, discussed in relation to the hypothesis of the accretion/merging origin of these galaxies.

Key words: galaxies: elliptical and lenticular — galaxies: interactions — galaxies: kinematics and dynamics

1. Introduction

We are investigating the star formation history of nearby early-type galaxies with fine structures. Galaxies are located in low density environments, i.e. shell galaxies are nearly isolated (Malin & Carter 1983) while pairs considered are typical inhabitants of the edges of super–clusters (see Karachentsev 1990). We wish to study the correlation between the star formation and the interaction events. The presence of fine structures in the main body morphology of the galaxies is widely believed to be a signature of such processes (see for a review Barnes & Hernquist 1992). In this paper we present the kinematics of the *stellar* and of the *gaseous* components of a sample of shell galaxies and pair members, whose spectro–photometric data have been presented in Longhetti et al. (1997a, Paper I).

Send offprint requests to: R. Rampazzo

⋆ Based on observations obtained at ESO, La Silla, Chile. Data and and kinematical profiles are available at CDS.

The present kinematic data have been used for the correction of the line–strength indices in Paper I. Furthermore, they permit the identification of "bona fide" signs of interaction. Encounters and kinematic signs among the pair member galaxies have been widely studied by Borne (1990 and reference therein) and Combes et al. (1995) using N-body simulations. Among the "bona fide" signs of interaction they consider the U-shape of the stellar velocity profile. They interpret the U-shape in terms of the ongoing ablation of the outer parts between members during the encounter. Models developed by these authors can make definite predictions about the physical reality of interacting pairs, i.e. if they form bound or unbound systems. Balcell & Quinn (1990) simulations found that the accretion of a small satellite may cause a well recognizable dip in the stellar velocity dispersion profile.

The indication coming from the kinematics of the ionized gaseous component concerning the degree of the interaction is still debated. E.g. the counter-rotation of the gaseous component with respect to the stellar one is interpreted by the models either as the debris of a small accretion event (see Barnes & Hernquist 1992) or as a sign of a "weak interaction" involving an inner disc (Hau & Thompson 1994). Following Phillips et al. (1986), the physical condition of the ionized gas component found in early-type galaxies could be interpreted into a LINER framework, i.e. from starbursts to AGN like objects (Ho 1996). Although the wavelength range covered by our data is limited to perform an accurate analysis of the relevant lines ratios through diagnostic diagrams, we attempt to investigate excitation level of the ionized gas of some objects. Since we are interested in the star formation history, gas physical conditions will also be discussed in this context.

The paper is organized as follows. Observations and data reduction are presented in Sect. 2. In Sect. 3 we discuss the comparison with the literature and individual results. In Sect. 4 the physical status of the gas and the presence of LINER activity is presented. Section 5 discusses the origin of the galaxies in terms of the merging hypothesis. Finally, we summarize our conclusions in Sect. 6.

2. Observations and data reduction

Long slit spectra have been obtained during three different runs at the 1.5 m ESO telescope equipped with a Boller & Chivens spectrograph and a 2048^2 (15 μm pixel) CCD camera.

The characteristics of the 21 shell galaxies, 30 pair members and 5 "template" galaxies belonging to the Gonzalez (1993: G93) sample are described in Tables 1, 2 and 3 of Paper I respectively. Observational conditions and spectral parameters for each of the runs are detailed in Tables 4 and 5 of Paper I. Table 5 of this latter reports: the object identification (1), the observing run (2), the slit position angle oriented NE (3), the exposure time (4), the spectrum quality (5) and the portion of the galaxy enclosed in $5''$ in terms of equivalent diameter $D_{\rm e}^{\rm B}$ i.e. the diameter enclosing half of the total light in the B–band taken from Lauberts & Valentijn (1989: ESO-LV).

Galaxy observations were split into consecutive exposures. We typically obtained three successive frames with the same position angle. Calibration frames (He–Ar lamp) were taken before and after each galaxy exposure to allow accurate wavelength calibrations. Each of the galaxy frames has been treated separately. Pre-reduction, cosmic-ray hits removal, wavelength calibration and sky subtraction have been performed using the IRAF package. Multiple spectra were then co-added before being analyzed with a Fourier-fitting code. The Fourier-Fitting technique (see Simien & Prugniel 1997) is similar to that of Franx et al. (1989) for the simultaneous determination of the velocity dispersion $\sigma(r)$, and the rotational velocity $V(r)$ at a distance r from the centre. A parameter $\gamma(r)$, related to the absorption-line contrast with respect to an approximation of the continuum (represented by a third-order polynomial fitting to the spectrum), is also determined. In order to enhance the S/N ratio, adjacent lines were averaged in the outer parts of the galaxies. For a spectrum at radius r, a weight was assigned to the neighboring lines ($r \pm \delta r$) entering the average: for this weight, a gaussian fall-off as a function of δr was chosen, with a FWHM value between 1 and 3 pixels ($0\farcs6$ and $1\farcs8$).

Basic data of the stellar kinematics, i.e. heliocentric recession velocity $V_{0,\rm hel}$, central velocity dispersion σ_0, and value of $\sigma_{5''}$ adopted for the correction of line strength indices in Paper I, are collected in Table 1. The value of $\sigma_{5''}$ has been obtained coadding spectra along the line perpendicular to the spectral dispersion, in the region between $-2\farcs5$ and $2\farcs5$ with respect to the galaxy centre. Table 2 summarizes the measured difference between the systemic velocity of pair members, ΔV, and the projected separation.

In Table 1, detected *emission lines* are also reported, and the measured EW's are listed in Table 4. EW's have been measured with the same procedure adopted for the atomic indices (see Paper I), using the spectral bandpasses listed in Table 3. Emissions were detected by direct inspection of the spectra, and in the uncertain cases only after coadding. A careful check of the lines positions was done after having redshifted their wavelength to the rest-frame. Profiles of the galaxies emission lines were fitted with a gaussian curve whose peak was taken as a measure of the lines centres and used to obtain the kinematics of the galaxies gas components. The approximation of a line with a gaussian profile is acceptable for all the measured cases with the only remarkable exception of IC 5063 (RR331a), where a second line component is visible in its profile at the centre of the galaxy (see next paragraphs). We estimate our precision in higher

S/N rows better than 10 km s^{-1}, while we rejected data with errors larger than 30 km s^{-1} (0.5 px). Only for ESO 2890150, ESO 2440120/ESO 2440121 (RR 24a/b), ESO 5450400 (RR 62a), ESO 3860040 (RR 278a) and IC 5063 (RR 331a), emissions are extended outside the galaxy centre and it has been then possible to measure a gaseous velocity profile. We obtained the gas velocity dispersion, corrected for the instrumental dispersions, only for the latter objects.

When characterized by "regular" shapes, the galaxies velocity profiles have been parametrized with a sigmoid along their major axis, in order to obtain the maximum value of the velocity rotation, $V_{\max}$. Actually, the majority of the objects shows not regular curves and their $V_{\max}$ value has been obtained simply fitting outer data with a line in both sides of the velocity profile. We are aware both of the uncertainty of the latter method and of the fact that the velocity curves reach only the nuclear parts of the galaxies. Table 5 summarizes the informations concerning the rotational support parameters.

3. Comparisons and individual results

The reliability of our reduction procedure was examined comparing our measurements with those derived by other authors. Comparisons with the literature are quite difficult both for the systemic velocity and for the central velocity dispersion. In particular, an accurate comparison with the central velocity dispersions from the literature is hard to achieve, given the wide range in effective spatial resolution, the overall quality of the data, the diverse techniques and instrumentations used in different studies.

The check of the systemic velocity determination is done mainly using the heliocentric optical, $V_{\rm opt}$, velocity value listed in RC3 (de Vaucouleurs et al. 1991) and that listed in Reduzzi & Rampazzo (1995: hereafter RR95), since these sources offer the largest intersection and homogeneity with our sample. RR95 atlas reports systemic velocities derived from ESO-LV (Lauberts & Valentijn 1989) up to dated with measures obtained from recent surveys (Fairall & Jones 1991; da Costa, private communication). A compilation of velocity dispersion measurements has been recently published by Prugniel & Simien (1996: PS96 hereafter). PS96 is then our source for the comparison between our measurements of the central velocity dispersions an those available in the literature.

Figure 1 shows the difference between our heliocentric systemic velocities and the corresponding values reported in RC3. Among 26 of the 29 galaxies in common, the mean difference (our - RC3) is -1 ± 32 km s^{-1}. In three cases there is a quite large difference between our measurements and $V_{\rm opt}$ from RC3, namely for NGC 7135, NGC 7284 and IC 5250. The heliocentric systemic velocity quoted in RC3 for NGC 7135 is 2050±35 km s^{-1}. Our value (Table 2) substantially agrees with 2718±30 km s^{-1} given in Tully (1988). NGC 7284 according to RC3 has a systemic velocity of 4544 ± 65 km s^{-1}. Our value is in good agreement with the value 4706 km s^{-1} reported in ESO-LV. Analogously, RC3 reports for IC 5250 a systemic velocity of 3509±37 km s^{-1} while ESO-LV and and Fairall & Jones (1991) report respectively 2947 and 3123 km s^{-1}, in agreement with our determination. A mean difference of 8± 38 km s^{-1} is found comparing our systemic velocities for 21 pair members and data from RR95. The scatter

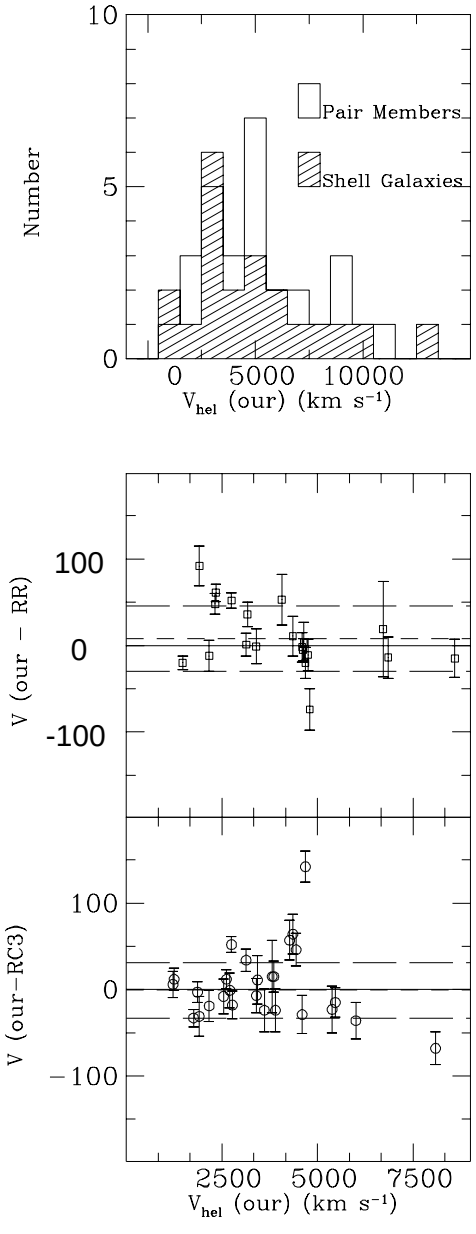

Fig. 1. (bottom panel) Comparison between our heliocentric systemic velocities and $V_{\rm opt}$ reported in RC3 for 26 common galaxies. (medium panel) The systemic velocity of pair members has been compared with literature data reported in RR95 catalogue. In both panels are plotted the average residual and the relative 1σ uncertainty. (upper panel) Systemic velocity distribution of pair members and shell galaxies

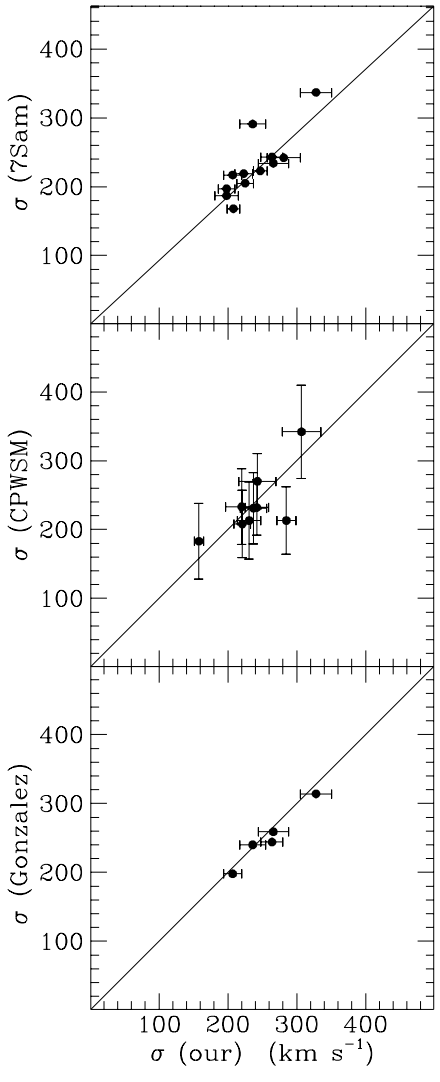

Fig. 2. Comparison between our values of nuclear velocity dispersion $\sigma_{5''}$ and those obtained by Gonzalez (1993: bottom panel), Carter et al. (1988: medium panel) and 7Sam (upper panel). In this latter panel our nuclear velocity dispersion for NGC 7785 and NGC 7619, the two upper points, disagree with the correspondent values adopted by 7Sam. These galaxies belong also to the set of G93 with which the agreement is quite good

with data from RC3 and from RR95 are probably due to the fact that part of the systemic velocity measurements comes from surveys which offer a lower precision than that obtained in detailed kinematic investigations. If we compare our systemic velocities to those obtained by Carter et al. (1988), a study dedicated to shell galaxies, we obtain a mean difference of -18 ± 15 km s^{-1} over 10 out of 11 common galaxies; only one object, namely E5390100, has a difference of 107 km s^{-1} with our estimate.

In Fig. 2, values of $\sigma_{5''}$ are compared with the two sets of data coming from G93 and Davies et al. (1987: 7Sam). Gonzalez's nuclear ($\sigma_{5''}$) velocity dispersions of the five galaxies in Table 1 compare within 9 ± 9 km s^{-1} with our measurements. G93 states that his nuclear velocity dispersions show a small positive offset when compared with 7Sam and Whitmore et al. (1985) data. At the same time, the average (our - 7Sam) difference of nuclear velocity dispersion is 10 ± 27 km s^{-1} among 12 common objects. Values of the central velocity dispersions, σ_0, are compared in the same figure with those obtained by Carter et al. (1988). The average difference (our - Carter et al.) is 2 ± 33 km s^{-1}. With respect to these authors, our kinematic zero point is then systematically positive by a very small factor, which anyway cannot affect the quality of the velocity dispersion correction applied to spectro-photometric data.

Velocity, $V_{\rm hel}$, and velocity dispersion, σ, curves as function of the distance from the centre are displayed in Figs. 3, and 4. In particular, Fig. 3 displays the comparisons with other authors for the 5 galaxies from the Gonzalez's (1993) set considered in Paper I as spectro-photometric templates. Detailed comparisons are discussed in the next subsections.

3.1. Individual notes and comparison with the literature for the galaxies in the G93 sample

NGC 584: Figure 3 shows the good agreement between our rotation and velocity dispersion profiles and those obtained by Davies & Illingworth (1983) along PA 63°. 7Sam adopted a central velocity dispersion of 217 km s^{-1} (raw data range between 215 and 245 km s^{-1}) in good agreement with our data reported in Table 1.

NGC 7562: Although in agreement within the errors, our value of the central velocity dispersion is ≈20 km s^{-1} higher than those obtained from Gonzalez (1993: 244 km s^{-1}) and 7 Sam (243 km s^{-1}).

NGC 7619: Figure 3 shows the comparison with Whitmore et al. (1987), Jedrzejewski & Schechter (1987) (PA = 34°) and Franx et al. (1989). Our data agree, within the errors, with both Jedrzejewski & Schechter (1989) and Franx et al. (1989). A zero point difference is evident, both in systemic velocity and velocity dispersion, with Whitmore et al. (1987) data. On the other side, the shape of their velocity profile is more similar to our one than that of Jedrzejewski & Schechter (1987) and Franx et al. (1989). Our central velocity dispersion is in agreement with that derived by 7Sam since their adopted value is 337 km s^{-1} (raw values range from 325 to 381 km s^{-1}).

NGC 7626: While our velocity curve is in agreement with that from both Jedrzejewski & Schechter (1989) (PA = 7) and Davies & Birkinshaw (1988) (PA = 4°), our velocity dispersion profile presents a small positive zero point shift with respect to that obtained by the latter authors. The central velocity dispersion adopted by 7Sam is 234 km s^{-1} (raw data range from 208 to 275 km s^{-1}). The average value in the literature (PS96) is σ_0=268 km s^{-1}, well in agreement with our estimate.

Table 1. Main kinematic data

Ident	$V_{0,\rm hel}$ km s^{-1}	σ_0 km s^{-1}	$\sigma_{5''}$ km s^{-1}	other ident.	Emission lines	Notes
NGC 584	1861±12	218±13	207±13			T
NGC 7562	3612±25	295±26	264±16			T
NGC 7619	3818±42	356±31	328±23			T
NGC 7626	3434±28	287±29	266±22			T
NGC 7785	3864±18	242±16	236±19			T
ESO 5390100	15803±54					S
ESO 2970340	5585±21	131±23				S
NGC 813	8092±19	209±24	208±19	ESO 0520160		S
NGC 1210	3904±25	219±27	180±16	ESO 4800310	[O II]	S
NGC 1316	1760±10	240±11	225±12	ESO 3570220	[O II] *	S
NGC 1549	1220±15	252±14	225±12	ESO 1570160		S
NGC 1553	1251±13	200±11	188±11	ESO 1570170		S
NGC 1571	4443±19	241±16	224±14	ESO 2500190		S
NGC 2865	2623±11	221±12	208±9	ESO 4980010		S
NGC 2945	4601±22	243±27	212±17	ESO 5650280	[O II]	S
NGC 3051	2544±20	237±19	212±18	ESO 4990160		S
NGC 5018	2776±16	285±14	247±10	ESO 5760100		S
NGC 6776	5465±17	231±17	243±13	ESO 1040530	[O II]	S
NGC 6849	6004±21	220±23	198±17	ESO 3390320		S
NGC 6958	2712±20	242±17	223±13	ESO 3410150	[O II]	S
ESO 1070040	3116±7	158±7	155±8			S
ESO 3420390	5384±27	307±28	327±21			S
NGC 7135	2640±21	202±21	191±16	ESO 4030350	[O II]	S
ESO 2890150	13327±112	274±32	161±94		[O II],Hβ	S
ESO 2400100(a)	3159±20	263±19	225±22			S
ESO 2400100(b)	3348±14	192±13	223±23		[O II]	S
ESO 5380100	9926±27	93±33	104±20			S
IC 1609	6918±22	223±22	214±17	ESO 2950260		S
ESO 2440120	6719±55	80±66	101±26	RR 24a	[O II], [O III], Hβ	P
ESO 2440121	6852±24	71±31	92±46	RR 24b	[O II], [O III], Hβ, Hγ	P
ESO 5450400	1474±8	67±11	81±9	RR 62a		P
ESO 4860170	4749±18	177±23	162±15	RR 101a	[O II]	P
ESO 4860190	4625±13	223±15	210±11	RR 101b		P
ESO 4860290	9923±29		130±33	RR 105a	[O II]	P
NGC 3289	2754±9	134±14	144±11	ESO 3750640,RR 187b		P
NGC 4105	1912±23	277±22	281±24	ESO 4400540,RR 210a	[O II]	P
NGC 4106	2170±18	253±17	212±12	ESO 4400560,RR 210b		P
ESO 5070450	4801±24	347±23	357±30	RR 225a		P
ESO 5070430	4600±17	196±16	186±13	RR 225b		P
ESO 3860040	4070±29		184±25	RR 278a	Hβ	P
ESO 2740060	4945±32	311±34	290±24	RR 282b		P
ESO 1380290	4641±23	199±27	205±16	RR 287a	[O II]	P
NGC 6734	4277±23	203±22	177±11	ESO 1040360,RR 297a		P
NGC 6736	4321±21	142±27	147±15	ESO 1040370,RR 297b		P
ESO 2830190	5805±35		92±37	RR 307a	[O II]	P

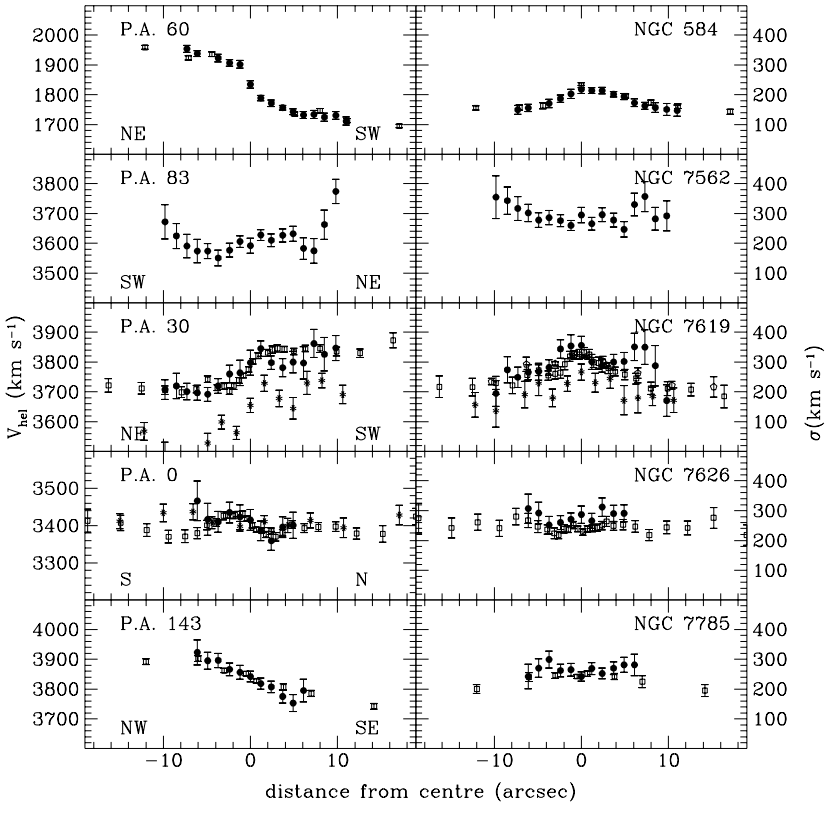

Fig. 3. Rotation (left panel) and velocity dispersion curves (right panel) as a function of the distance from the centre for the set of galaxies used as spectro-photometric templates. Comparisons between our measurements (full dots) and the data available in the literature are also shown. NGC 584: Davies & Illingworth (1983: open squares); NGC 7562, NGC 7619: Whitmore et al. (1987: asterisks), Jedrzejewski & Schechter (1989: open squares), Franx et al. (1989: open pentagons); NGC 7626: Jedrzejewski & Schechter (1989: open squares), Davies & Birkinshaw (1988: asterisks); NGC 7785: Bender et al. (1994: open squares)

Table 1. continued

Main ident.	$V_{0,\rm hel}$ km s^{-1}	σ_0 km s^{-1}	$\sigma_{5''}$ km s^{-1}	other ident.	Emission lines	Notes
ESO 2830200	5672±26	236±25	230±21	RR 307b		P
ESO 4000290	2325±12	176±13	189±11	RR 317a		P
ESO 4000300	2342±10		91±55	RR 317b		P
IC 5063	3401±20	165±23	153±32	ESO 1870230,RR 331a	[O III], Hβ, Hγ, Hδ, Hϵ	P
NGC 7284	4686±18	270±23	276±16	ESO 5330310,RR 381a		P
NGC 7285	4358±23	172±28		ESO 5330320, RR 381b		P
IC 5250	3169±14	200±14	187±11	ESO 1090220,RR 387a		P
ESO 1090221	3189±13	218±16	215±15	RR 387b		P
IC 5328	3137±13	207±13	198±12	ESO 2910280,RR 397b	[O II]	P
IC 5358	8044±29	188±31	192±23	ESO 4710190,RR 405a		P
ESO 4710191	8592±22	217±30	207±19	RR 405b		P
IC 5364	8849±41	177±55	187±35	ESO 4710470,RR 409a		P
ESO 4710471	9155±33	126±45	150±25	RR 409b		P

T stands for "template galaxy", **S** for "shell galaxy" and **P** for "pair member". [O II] refers to the detection of 3727−3729 Å lines, [O III] to 4958 and 5007 Å lines. E 2400100 has two distinct nuclei in the spectrum which are indicated as **a** and **b** (see also the text and Fig. 4.4). The spectrum of E 5390100 is very faint and it was not possible to obtain reliable velocity dispersion measurements. Lines indicated with an asterisk are very weak respectively. IC 1609 is not part of the spectrophotometric sample analyzed in Paper I.

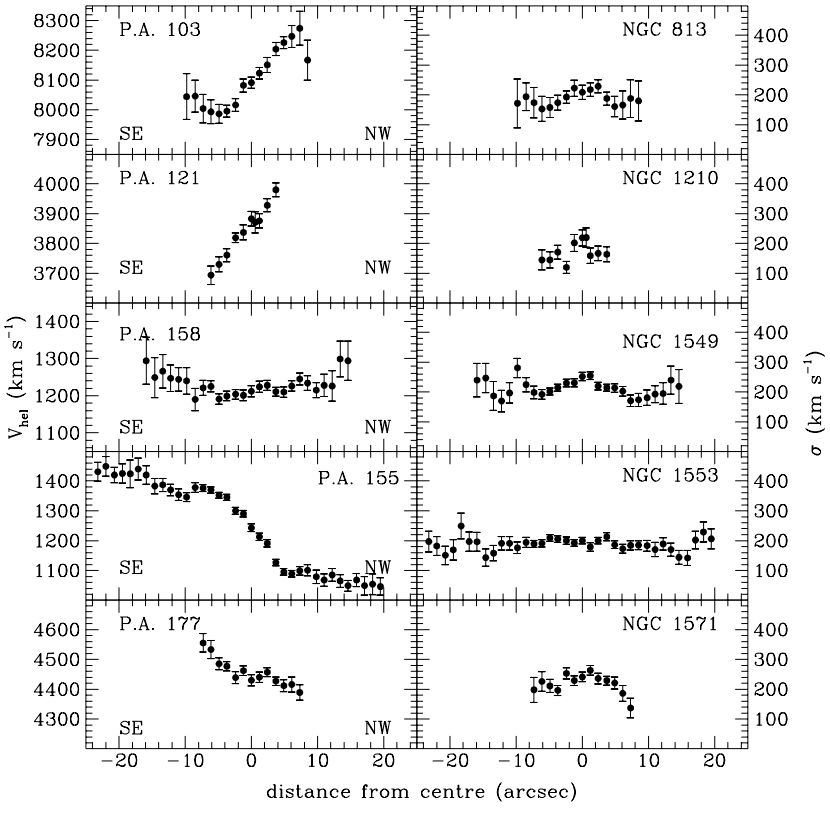

Fig. 4. 1. Rotation (left panel) and velocity dispersion curves (right panel) as a function of the distance from the galaxies centre for the shell objects sample. Full circles mark the stellar component. Open symbols indicate the gaseous component as determined by Hβ 4861 Å line (squares), [O III] 4959 Å line (triangles) and [O III] 5007 Å line (pentagons)

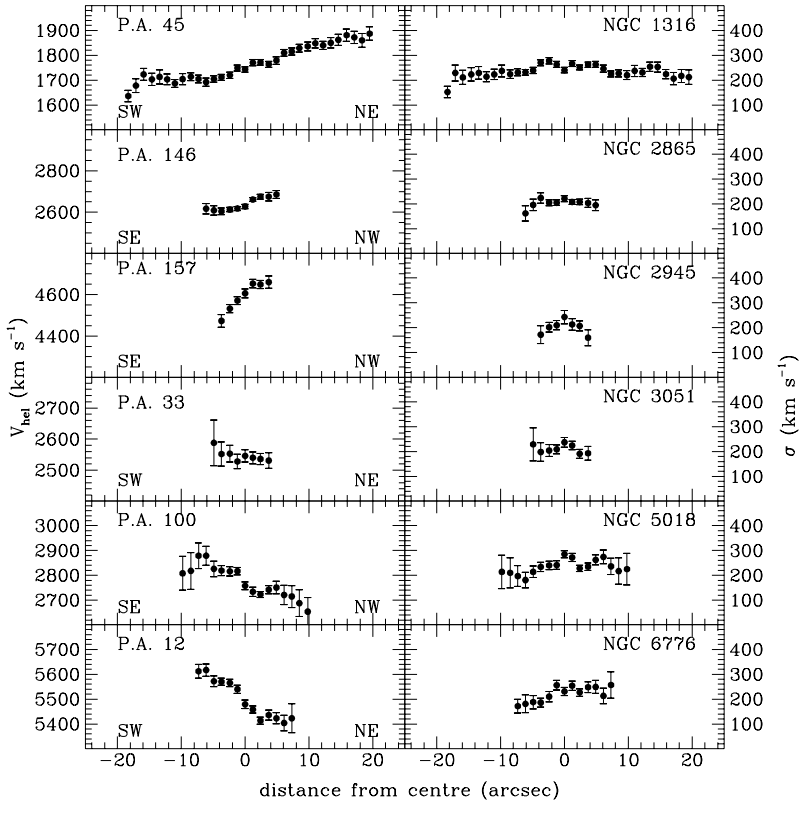

Fig. 4. 2. See Fig. 4.1

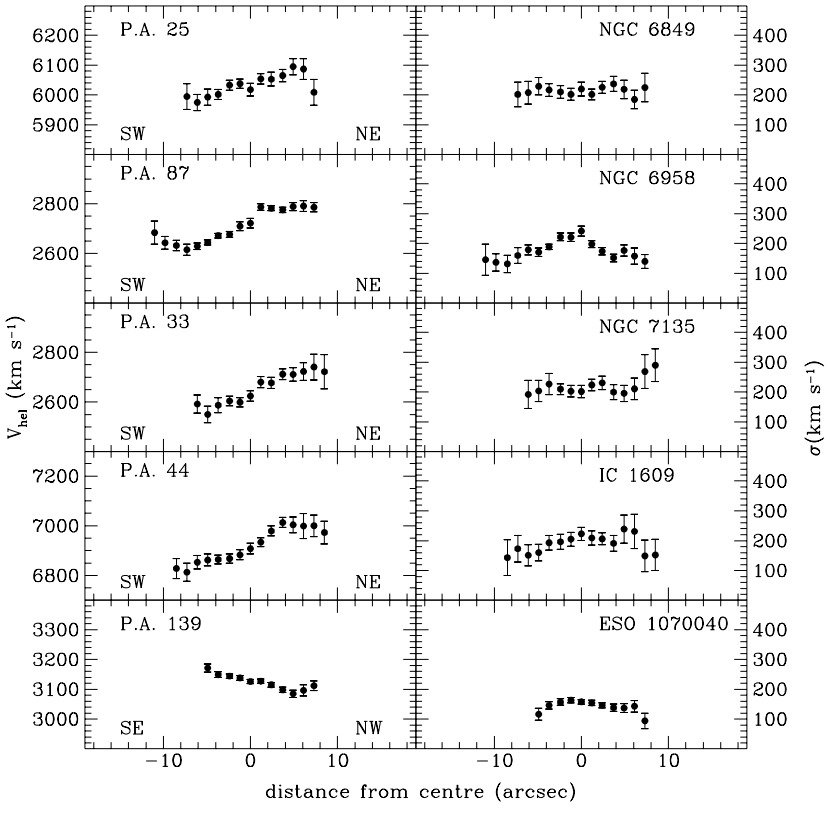

Fig. 4. 3. See Fig. 4.1

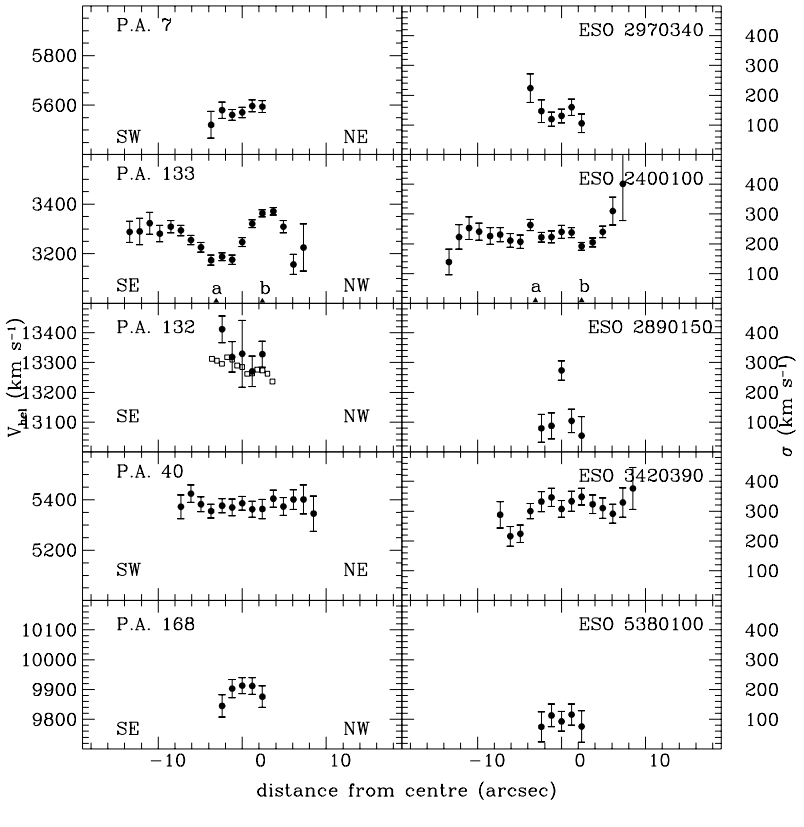

Fig. 4. 4. See Fig. 4.1

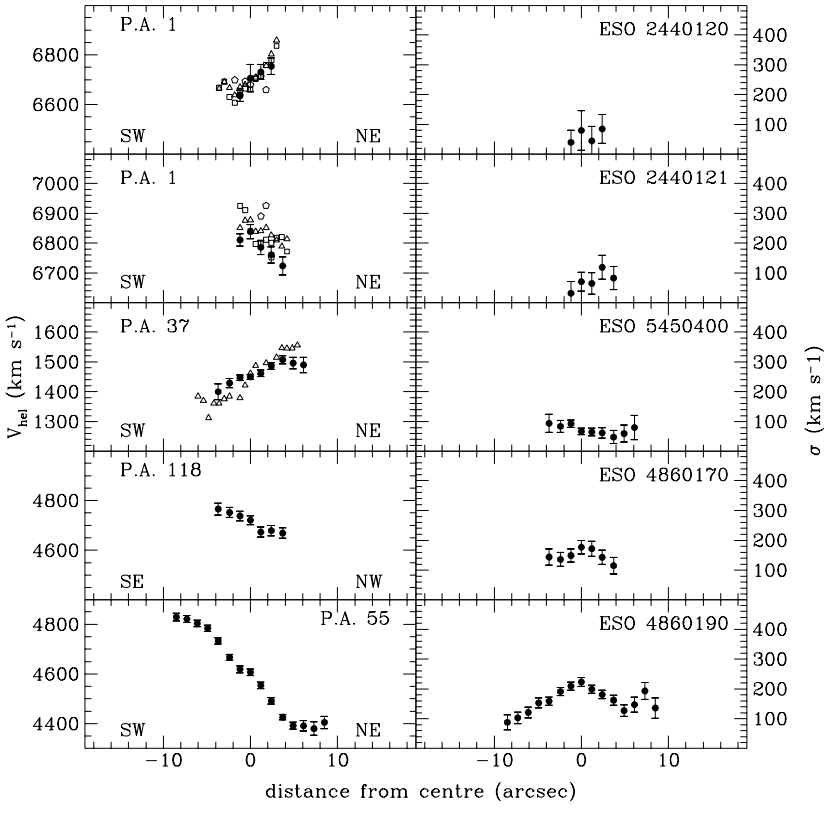

Fig. 4. 5. Rotation (left panel) and velocity dispersion curves (right panel) as a function of the distance from the galaxies centre for the pair sample. Symbols are the same as in Fig. 4.1

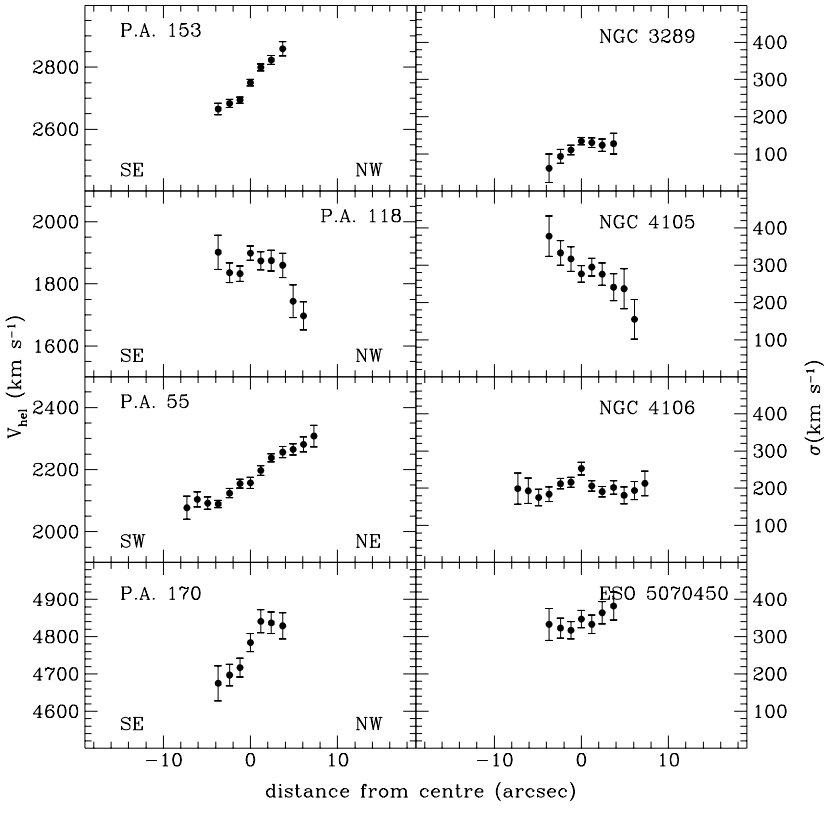

Fig. 4. 6. See Fig. 4.5

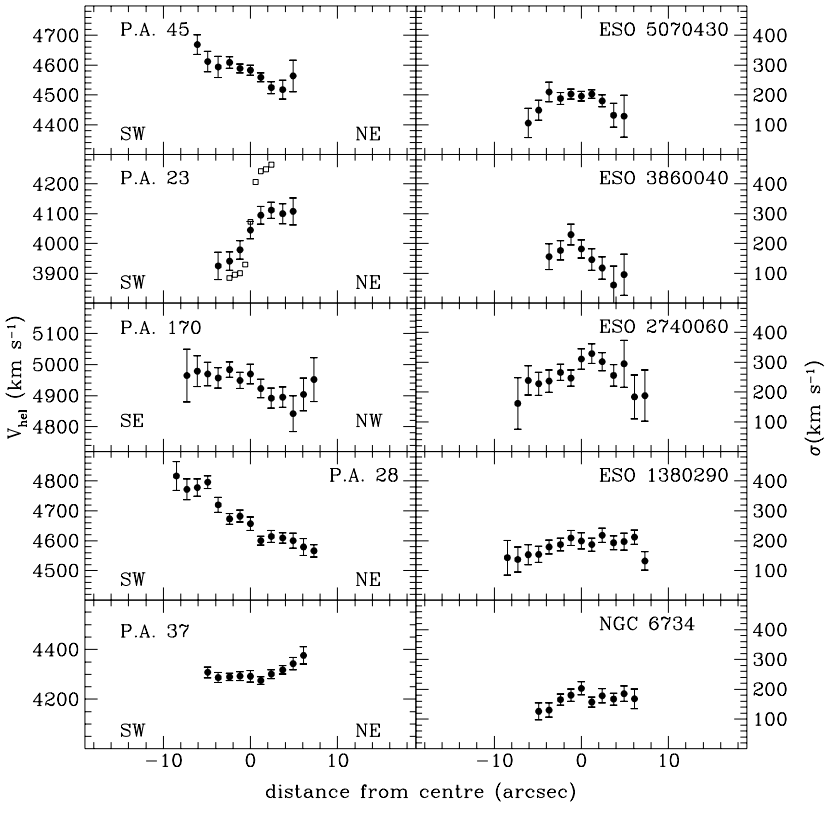

Fig. 4. 7. See Fig. 4.5

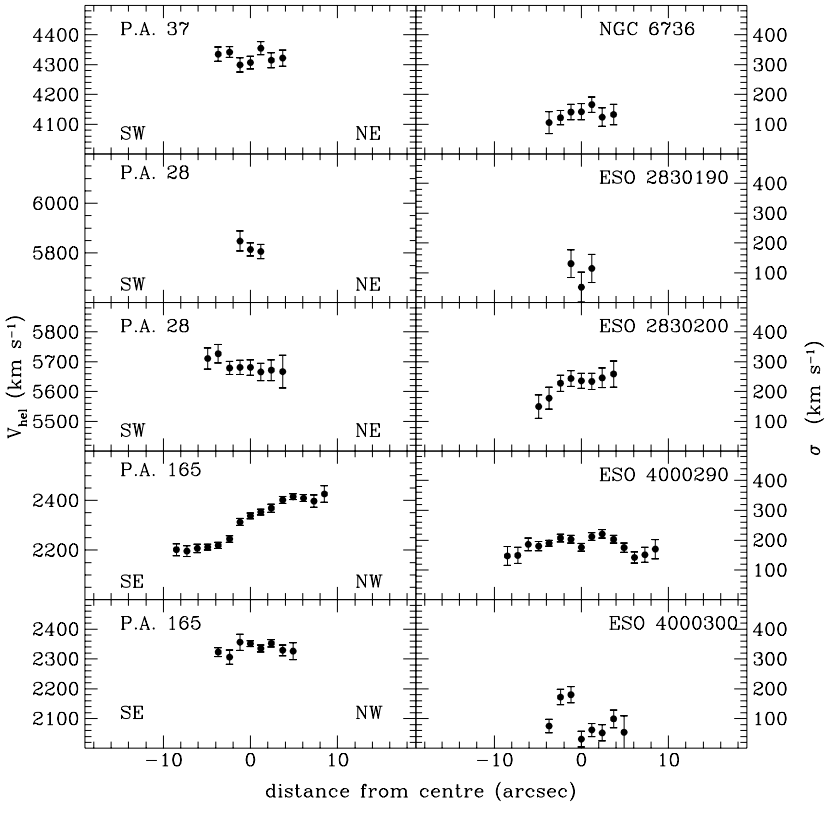

Fig. 4. 8. See Fig. 4.5

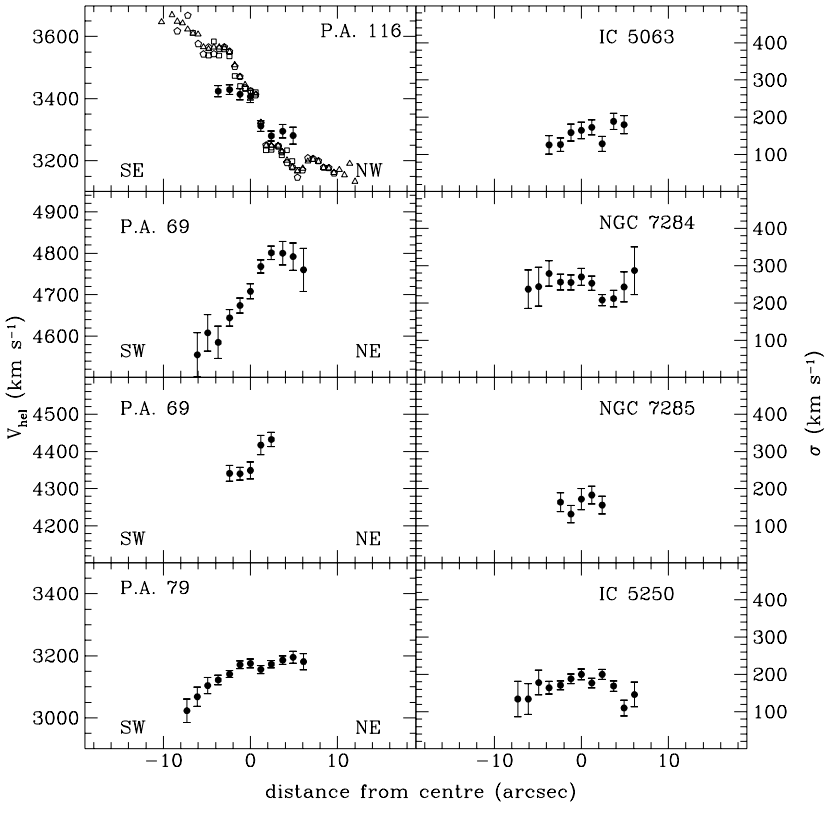

Fig. 4. 9. See Fig. 4.5

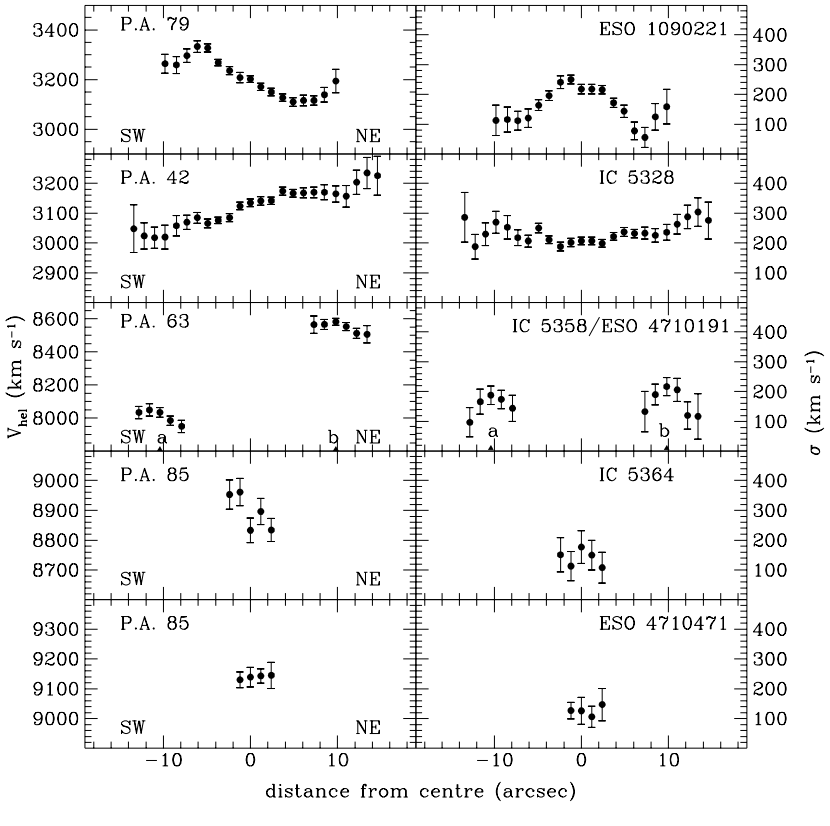

Fig. 4. 10. See Fig. 4.5

Table 2. Futher information on pairs

Ident	ΔV km s^{-1}	Sep. ($'$)
RR 24	133	0.3
RR 62		1.7
RR 101	124	1.6
RR 105	196	1.6
RR 187		2.7
RR 210	258	1.0
RR 225	201	2.2
RR 278	373	3.6
RR 282		5.3
RR 287		2.9
RR 297	44	2.6
RR 307	133	2.3
RR 317	17	1.1
RR 331	39	10.9
RR 381	328	0.5
RR 387	20	0.5
RR 397	961	0.8
RR 405a	546	0.4
RR 409a	306	0.3

NGC 7785: Bender et al. (1994) have obtained for this galaxy rotation and velocity dispersion profiles along a PA = 138°. Figure 3, in which the comparison with our measurements is shown, indicates a good agreement between the two sets of data. 7Sam adopted value of the central velocity dispersion, 291 km s^{-1} (raw value 299 km s^{-1}), is the highest in the literature.

3.2. Individual notes and comparison with the literature for shells galaxies

In the Figs. 4.1-4, the velocity and velocity dispersion curves of the shell galaxies are presented. Note that the shell galaxy IC 1609 is not part of the spectrophotometric sample analyzed in Paper I.

NGC 1316: Schweizer (1981) studied the optical properties of the NGC 1316 core obtaining an estimate of the central velocity dispersion of 248±6 km s^{-1}. Both this value and the average one in the literature (250 km s^{-1}, PS96) are in agreement with our measure.

NGC 1549: This galaxy is interacting with NGC 1553 (Malin & Carter 1983). The galaxy geometry is characterized by a strong twisting (Rampazzo 1987) and shows significant rotation along different axes (Rampazzo 1988; Franx et al. 1989). PS96 report 213 km s^{-1} as the average value in the literature for central velocity dispersion, in good agreement with our nuclear value.

NGC 1553: Differently from the companion NGC 1549, the geometry of NGC 1553 is characterized by a nearly constant position angle. The extended velocity curves studied by Kormendy (1984) and Rampazzo (1988), along PA = 149.°5 and PA = 140° respectively, show a secondary maximum (≈ at 10″), visible also in our velocity curve. No rotation is measured by the previous authors along the minor axis (PA = 59.°5; PA = 50° axes respectively) confirming that NGC 1553 is a lenticular galaxy. PS96 report 185 km s^{-1} as the average value in the literature for the central velocity dispersion, in good agreement with our nuclear value.

NGC 2865: Bettoni (1992) has obtained the velocity curve (PA = 150) and the central velocity dispersion for this galaxy. The velocity profile obtained by the previous author is in good agreement with our measurement. This galaxy shows a large external complex of HI (Schiminovich et al. 1995) with a systemic velocity of 2640±15 km s^{-1} well in agreement with our determination for the stellar component. Stars and gas seem then to be associated and co-rotating, as outlined by the previous authors. Our value of the central velocity dispersion is in agreement with the Carter et al. (1988) value of 208±46 km s^{-1}. Lower values, although in agreement within the errors, are given by Bettoni (1992) 180±24 and 7Sam whose adopted value is 168 km s^{-1} (raw data range from 161 to 199 km s^{-1}).

NGC 5018: The galaxy has been recently observed by Carollo & Danziger (1993) along both the major (PA 99°) and minor (PA 9°) axis. Our rotation and velocity dispersion curves agree with their ones. In particular the velocity dispersion curve shows a deep of ≈ 50 km s^{-1} slightly displaced (1.″8) from the centre. Carollo & Danziger (1993) model the dynamics of NGC 5018 suggesting that velocity and velocity dispersion curves are well fitted by an oblate rotator, with a flat diffuse dark halo 3 times as large as the luminous component.

NGC 6849: The galaxy shows a regular rotation (≈75 km s^{-1}) along the major axis. The velocity dispersion curve is flat. The σ average value in the literature (PS96) is 211 km s^{-1} in agreement with our measures.

E 2890150: Stellar and gaseous components (the latter studied through the Hβ emission) co–rotate, and their systemic velocities are in agreement within the errors, which for the stellar component are quite large. The average gas velocity dispersion is 82±59 km s^{-1}.

E 2400100: Our spectra (three independent observations) show two distinct components whose centres are indicated in Fig. 4.4 as **a** and **b**. The two components are separated by ≈ 5″ and 200 km s^{-1} in the redshift space. In the previous papers (Malin & Carter 1983; Carter et al. 1988) dealing with this object, this characteristic has not been noticed. While it is not surprising in the case of the Malin & Carter catalog, since it is obtained from very deep Schmidt plates, the fact that Carter et al. (1988) did not notice a double nucleus could be explained by a different slit PA In fact, our measure of the nuclear systemic velocity and of the velocity dispersion on the main body of

the galaxy are in good agreement with those derived by Carter et al. (1988).

3.3. Individual notes and comparison with the literature for pairs members

Reduzzi & Rampazzo (1996: R&R96 hereafter) have obtained the B, V, R surface photometry of most of the present sample pairs. In R&R96 Table 4, informations about the galaxies inner fine structure and possible morphological misclassification on the basis of luminosity, geometric and color profiles are also given. The Figs. 4.5-4.10 report the velocity and velocity dispersion curves for this part of the sample. Note that ESO 4860290 (RR 105a) data are not riported in Fig. 4 because we obtained only the central kinematic for this object whose observations are characterized by a low S/N ratio. For completeness we have included ESO 5330320 (RR 381b), although it is not part of the spectrophotometric sample analyzed in Paper I.

ESO 2440120/121 (RR 24): Both the galaxies have a very distorted morphology (R&R96), showing long, asymmetric tails/arms. ESO 2440120/2440121 are classified as a spiral and a late S0. The $(B-V)$ color map is consistent with the late-type classification. In the present sample they represent the objects with the latest morphological type and nuclear indices refer to their bulges. The gas velocity curve of ESO 2440120 (RR 24a) is consistent with that of the stars, while in ESO 2440121 (RR 24b), although having the same slope, the two components differ in the systemic velocity. Velocity dispersion is very small at the limit of our resolution.

ESO 5450400 (RR 62a): ESO-LV classification of this galaxy reports it as an S0 object, but the luminosity profile is well fitted by a $r^{1/4}$ law (R&R96). $(B-V)$ color profile is consistent with an early-type galaxy.

NGC 4105/4106 (RR 210): Pair members are strongly interacting. This is visible both in the velocity and in the velocity dispersion curve of NGC 4105 (RR 210a) obtained at PA 118, i.e. along the line connecting the two nuclei. The velocity curve of RR 210a could be interpreted in the framework of U-shape profiles. The axis along which NGC 4106 (RR 210b) has been observed is less contaminated by the interaction and shows a nearly normal rotation and velocity dispersion profile. NGC 4106 is a fast rotator: the peak velocity up to the last observed point is 116 km s^{-1}.

ESO 3860040 (RR 278a): This galaxy is a lenticular. R&R96 found shells and dust in this galaxy. Measurements, done on independent parts of the spectrum, suggests that gas has a steeper rotation curve than stars, although in the same sense. This could be interpreted within the framework in which the stellar and gaseous components lie in different planes as already reported in other remarkable cases (Galletta 1996; Plana & Boulesteix 1996). In the central 2.″4 the velocity dispersion of the gas is 171 km s^{-1} similar to the stellar one. It is quite difficult, without further studies, to understand the origin of the gas, which could e.g. has been accreted from the spiral companion or, having lost angular momentum during the interaction, to be conveyed from the galaxy outskirts to the centre.

Table 3. Definitions of the emission lines bandpasses

Index	Central bandpass [Å]	Continuum bandpass [Å]
Hβ	4851.32 − 4871.32	4815.00 − 4845.00
		4880.00 − 4930.00
[OIII](4959Å)	4948.92 − 4978.92	4885.00 − 4935.00
		5030.00 − 5070.00
[OIII](5007Å)	4996.85 − 5016.85	4885.00 − 4935.00
		5030.00 − 5070.00
[OII](3727Å)	3720.00 − 3737.00	3706.00 − 3716.00
		3740.00 − 3760.00

Note: with the only exception of the [OII](3727 Å) line, all the spectral bandpasses are taken from G93.

4. Presence of nuclear activity

8 (1 uncertain) out of 22 shell galaxies nuclei show emission lines, most of which (7 out of 22) are [OII] lines. In E 2890150 ($T=-2$) is visible only Hβ.

Among pair galaxies, 10 objects out of 30 show emission lines. Together with [OII] lines as in the case of shell galaxies, [OIII] (4958 and 5007 Å) and Balmer lines (Hβ, Hγ and Hδ) are also frequently detected. The detection includes all galaxies with latest morphological types i.e. RR 24b ($T=3$), RR 24b ($T=-0.3$), RR 62a ($T=-2$) and RR 331a ($T=-0.4$) for which the gas presence is reasonably expected.

Phillips et al. (1986) found, among early-type galaxies, a large presence of nuclei which are indinstingushable from a LINER. Ho (1996) suggests that it is not convenient to classify activity only on the base of ([N II] λ6583)/ Hα) lines ratio, as in the case of Phillips et al. (1986), since the latter cannot give useful informations about the excitation level in galaxies. The original definition of a LINER, given by Heckman (1980), requests that the emission line ratios ([O II λ 3727)/([O III] λ 5007) is ≥ 1 and that ([O I λ 6300)/([O III] λ 5007) is ≥ 1.3. Veilleux & Osterbrok (1987) proposed other criteria for the LINER definition, among which the request that the ratio of ([O III] λ 5007)/Hβ is ≤ 3.

Our spectral range does not extend enough in order to compute several lines ratios and to use diagnostic diagrams (e.g. Veilleux & Osterbrok 1987). We use

Table 4. Emission lines EW

Ident.		[OII](3727)		[OIII](4959)		[OIII](5007)		Hβ	
ESO 2440120	P	18.02	± 1.47	2.17	± 0.16			2.35	± 0.11
ESO 2440121	P	34.05	± 0.82	4.27	± 0.18	2.63	± 0.14	16.13	± 0.16
ESO 4860170	P	16.24	± 1.62						
ESO 4860290	P	6.73	± 1.85						
NGC4105	P	18.09	± 10.59						
ESO 3860040	P							1.61	± 0.15
ESO 1380290	P	14.96	± 2.49						
ESO 2830190	P	30.70	± 8.79						
ESO 4000290	P	13.01	± 2.39						
ESO 1870230	P			75.47	± 0.32	45.90	± 0.21	22.11	± 0.16
IC 5328	P	3.73	± 0.39						
NGC 6776	S	2.45	± 0.24						
NGC 7135	S	10.75	± 0.70						
NGC 1210	S	7.09	± 1.34						
NGC 1316	S	1.67	± 0.38						
NGC 6958	S	3.60	± 0.19						
NGC 2945	S	24.38	± 1.41						
E 2890150	S							*	
E 2400100b	S	6.04	± 0.61						

Note: **S** stands for "shell galaxy" and **P** for "pair member". E 2890150 shows a detectable Hβ emission (see Fig. 6 in Paper I), but it cannot be measured through the standard wavelenght windows because it is inserted in a very deep absorption feature.

([O III]λ 5007)/Hβ line ratio in order to measure the nucleous ionization level and for 6 objects, belonging to the shell galaxies sample we attempt a first classification of the nuclear activity using ([N II]/ Hα) line ratio reported in Phillips et al. (1986). 4 shell galaxies (NGC 1316, NGC 1553, NGC 6776 and NGC 6958) out of 6 may be classified as LINERs on the basis of ([N II]/ Hα) vs. ([O III]λ 5007)/Hβ diagnostic diagram. The remaining two objects (NGC 1549, companion of NGC 1553, and NGC 1571) do not present LINER properties. E 2890150 shows ([O III]λ 5007)/Hβ line ratio that suggests the presence of a low excitation region, probably typical of the HII regions.

RR 24a/b are in the regime of low excitation. The ([O III] λ 5007)/Hβ ratio for RR 331a suggests that the nucleous is in the ionization regime of Seyfert galaxies. The ([O III] λ 5007) line profile as function of the radius, shown in Fig. 5 adds further evidence to this conclusion showing a double component. In a recent study of Aoki et al. (1996), [OIII] emission line shows the same behaviour in the nuclear region of the Seyfert galaxy NGC 7319.

We conclude that a small fraction of the studied objects may be classified as LINERs.

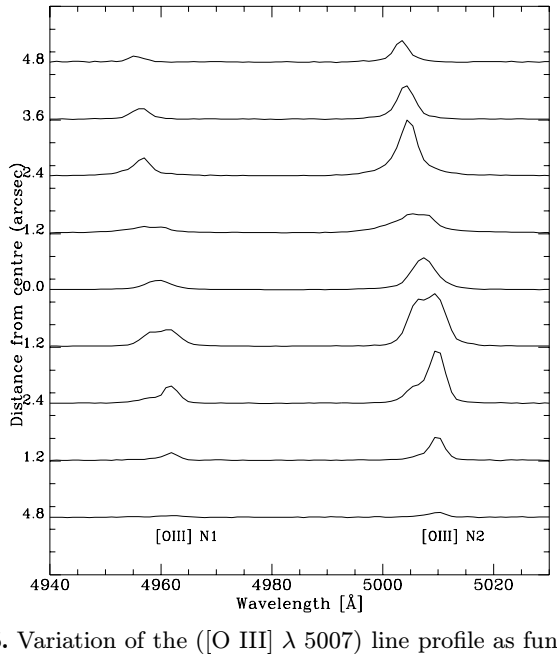

Fig. 5. Variation of the ([O III] λ 5007) line profile as function of the distance from the centre ($r = 0$) of RR 331a. Notice the double component in the central lines

5. Do shell galaxies have the kinematic structure of merger remnants?

The shell structure is widely indicated as a signature of a merging event, (see Barnes & Hernquist 1992 and reference therein). On the contrary, Thomson (1991) suggests

Table 5. Rotational support parameters for the stellar component for galaxies with unperturbed curve along their major axis

Ident	$V_{\rm max}^{\rm star}$ km s^{-1}	$r_{\rm max}$ (arcsec)	$r_{\rm ext}/r_{\rm e}$ (arcsec)	ϵ	$V_{\rm max}^{\rm star}/\sigma_{5''}$	$V_{\rm max}^{\rm gas}$ km s^{-1}	Notes
NGC 584	110	5	0.40	0.30	0.53		T
NGC 7562	<50		0.45	0.29	<0.19		T
NGC 7619	>68	10	0.28	0.24	>0.21		T
NGC 7626	<40		0.16	0.13	<0.15		T
NGC 7785	>65	7	0.30	0.42	>0.28		T
NGC 813	>165	6	0.59	0.32	>0.79		S
NGC 1210	>129	6	0.34	0.14	>0.72		S
NGC 1316	88	10	0.14	0.29	0.39		S
NGC 1549	<100		0.29	0.10	<0.44		S
NGC 1553	178	14	0.40	0.35	0.95		S
NGC 1571	<80		0.59	0.21	<0.36		S
NGC 2865	>40	6	0.37	0.16	>0.19		S
NGC 2945	>40	4	0.40	0.08	>0.19		S
NGC 3051	<15		0.20	0.11	<0.07		S
NGC 5018	90	5	0.47	0.28	0.36		S
NGC 6776	>103	7	0.50	0.15	>0.42		S
NGC 6849	>104	8	1.45	0.32	>0.53		S
NGC 6958	>82	10	0.46	0.15	>0.37		S
ESO 1070040	>34	5	0.44	0.11	>0.22		S
ESO 3420390	<20	8	0.24	0.40	<0.6	95	S
NGC 7135	78	5	0.11	0.32	0.41		S
IC 1609	>80	8	0.53				S
ESO 5450400	>50	6	0.48	0.34	>0.62		P
ESO 4860190	249	8	1.90				P
NGC 3289	>98	4	0.12	0.65	>0.6		P
NGC 4106	>120	8	0.14	0.45	>0.57		P
ESO 5070450	>69	4	0.20	0.28	>0.19		P
ESO 5070430	>60	6	1.05		>0.16	0.32	P
ESO 3860040	83	5	0.53	0.30	0.45	190	P
ESO 2740060	35	2	0.75	0.32	0.12		P
ESO 1380290	>100	8	0.26	0.51	>0.49		P
IC 5063	67	3	0.20	0.24	0.44	250	P
NGC 7284	112	6	0.26	0.21	0.41		P
IC 5250	>80	8	0.26	0.60	>0.43		P
ESO 1090221	110	6	0.30	0.57	0.51		P
IC 5328	>98	10	0.52	0.36	>0.49		P

$V_{\rm max}^{\rm star}$ is the maximum value reached in the stellar velocity profile and $r_{\rm max}$ is the corrisponding distance from the centre, while $r_{\rm ext}/r_{\rm e}$ is the extension of the curve in effective radius unit. We use ">" before the $V_{\rm max}^{\rm star}$ value when the trend of the velocity profile is still increasing at $r_{\rm ext}$ and when it is characterized by asymmetries, e.g. one side is flat an the other increasing at $r_{\rm ext}$. At the opposite, < indicates that the estimate of $V_{\rm max}^{\rm star}$ is an upper limit whithin $r_{\rm ext}$. The value of the effective radius in the B-band, $r_{\rm e}$, is obtained from ESO-LV, with the only exception of the 5 "template" galaxies for which we use RC3 data. The average ellipticity, ϵ, is obtained from G93 for the 5 "template" galaxies, while the remaninig values are from ESO-LV. The legenda in the column of notes is the same as Table 1.

that a "weak intercation" may produce long lasting shells. Both hypotheses explain several properties of the shells and of the host galaxy.

As discussed above, in E 2400100 two nuclei are visible. Borne (1990 and references therein) and Combes et al. (1995) have simulated interpenetrating encounters of two galaxies showing that a "bona fide" indication of the ongoing interaction is U-shape (and the correlated inverse U-shape) of the stellar velocity profile. In our view, the velocity profile of the two components in E 2400100 is an example of this behaviour. The velocity dispersion curve is asymmetric, showing a rapid rising (although with large uncertainties) in the NW part of the galaxy. The U-shape profile is developed both during bound and during unbound encounters (see Borne 1990); so it is difficult on this basis to know the dynamical evolution of E 2400100. If this object represents the final phase of an encounter, when the two galaxies are going to coalesce, and if the formation of shells in the galaxy is the results of such an encounter, these structures have to be very recent, since we still distinguish the two nuclei of the progenitors.

Recently Heyl et al. (1996) performed numerical experiments in order to identify kinematical signatures of "old" merging events in elliptical galaxies. The basic idea is that during a merging process there is a significant outward of angular momentum transfer. This will end in a merger remnant which will be supported by random motion in the centre but characterized by rapid rotation in the outer portions. This translates directly in a V/σ increase with respect to the radius, up to 0.5 in the outskirts. This evidence adds to the kinematic misalignments noticed in the simulated merger remnants. Both these characteristics are not present when the galaxy formation takes place through hierarchical collapse (Warren et al. 1992). We have calculated the V/σ ratio for some of the sample galaxies, and their trends indicate different conditions in the galaxies nuclei. E 3420390 is dominated by anisotropy just like the nuclear parts of NGC 1549 and NGC 2865. Velocity curves available in the literature for NGC 1549 (Rampazzo 1988; Franx et al. 1989), which extend in radius up to $\approx 1\ r_{\rm e}$, indicate that V/σ grows at ≈ 0.5. In this galaxy, kinematic misalignments (rotation along apparent minor axes, strong twist of isopothes $> 120°$) are further noticed. For NGC 2865 too, stellar kinematics data of Bettoni (1992) suggest an increase of V/σ up to $1.3 - 1.4$ in the outer parts. The HI gas detection extend further out the kinematics, showing an increase in the rotation velocity. The lack of gas in the central part of this galaxy has led Schiminovich et al. (1995) to consider the hypothesis that it has been converted to stars through a starburst. In Paper III we suggest, on the ground of spectrophotometric models, that a burst can be happened in the centre of this galaxy about 2 Gyr ago (depending on the selected models).

NGC 6776, NGC 813, NGC 1316 and NGC 1553 are in the range of oblate rotators. The kinematical and structural differences between the two companion galaxies NGC 1549, NGC 1553 are particularly significant. Differently from NGC 1549, NGC 1553 does not rotate along the minor axis (Kormendy 1984; Rampazzo 1988) and the isophotal twisting is $\leq 2°$ (Rampazzo 1987). For both these shell galaxies spectro–photometric models suggest that the last episode of star formation is quite old (see Paper III).

6. Conclusions

We presented the kinematics of the stellar and gaseous components in 51 galaxies. The sample is composed of 5 elliptical galaxies in the G93, considered spectro–photometric template in Paper I, 21 shell galaxies (22 nuclei) and 30 pair members. With the exclusion of RR 24b, all the galaxies have morphological type $T < 0$. Galaxies in the sample are located in low density environments and most of pair members show fine structures reported in Paper I.

The systemic velocity and central velocity dispersion characterizing the stellar kinematics of the more luminous galaxies in the sample are in good agreement with previous investigations, with few exceptions. A remarkable one concerns E 2400100 whose spectrum shows two distinct nuclei, not previously noticed, embedded in the main body of the galaxy. The shape of the composite velocity profile this galaxy may be interpreted in the framework of the U-shape profiles discussed by Combes et al. (1995).

V/σ as a function of radius shows a manifold of trends in the central parts of the shell galaxies. If shell galaxies have suffered a merging according to Heyl et al. (1996) we should find basically random motion in the center and rotation in the outskirts, since a significant outward angular momentum transfer is foreseen during a merging process. The manifold of trends noticed suggest that different mechanisms could be involved in the shells formation.

A small fraction of the objects show emission lines; in few of them, most of which are pair members, gas emission is extended. None of the objects in the sample shows counter-rotation of the gaseous versus the stellar component. On the contrary, we found cases in which the two components are associated. In two cases there is evidence that gas and stars lie on different planes. This latter phenomenon could be associated to accretion events.

From the ratio ([O II]/Hβ) we deduce that the physical condition of the gas in RR 331a is typical of a Seyfert. A double component visible in the line profile in the nucleus further supports this hypothesis which needs to be confirmed using wider spectral ranges. Evidence about the presence of a LINER nucleus in 4 galaxies belonging to the shells sample has been addressed using ([N II]/ Hα) emission lines ratio obtained by Phillips et al. (1986). It remains unexplained what are the mechanism/s generating the LINER activity (e.g. shoch waves, starburst, HII

region plus a low level nuclear activity, etc.). Other shell galaxies showing ([O II] λ 5007) could be in the regime of normal HII regions or belong to a a class of "transition" objects (as defined by Ho 1996), which lie in between HII regions and LINERS: a larger spectral range is necessary in order to classify them. From the line profile we have not indication of the presence of a broad component, which can be directly linked to the classical Seyfert galaxy type or to any kind of nuclear activity.

Acknowledgements. We wish to thank Francois Simien who permitted us to use his Fourier Fitting package and Daniela Bettoni and Giuseppe Galletta for tests made with their FQ package. ML acknowledges the kind hospitality of the Brera Observatory and of the Padova Observatory during her PhD Thesis. ML, AB and CC acknowledge the support by the European Community under TMR grant ERBFMRX-CT96-0086.

References

Aoki K., Ohtani H., Yoshida M., Kosugi G., 1996, AJ 111, 140
Balcells M. Quinn P.J., 1990, ApJ 361, 381
Barnes J.E., Hernquist L.E., 1992, ARA&A 30, 705
Bender R., Saglia R.P., Gerhard O.E., 1994, MNRAS 269, 785
Bettoni D., 1992, A&AS 96, 333
Borne K.D., 1990, in Dynamics and Interaction of Galaxies, Wielen R. (ed.). Springer-Verlag, p. 196
Carollo C.M., Danziger I.J., 1993, in Structure, Dynamics and Chemical Evolution of Elliptical galaxies, Danziger I.J., Zeilinger W.W. and Kjär K. (eds.). ESO/IPC, p. 431
Carter D., Prieur J.L., Wilkinson A., Sparks W.B., Malin D.F., 1988, MNRAS 235, 813
Combes F., Rampazzo R., Bonfanti P., Prugniel Ph., Sulentic J.W., 1995, A&A 297, 37
Davies R.L., Illingworth, 1983, ApJ 266, 516
Davies R.L., Burstein D., Dressler A., et al., 1987, ApJS 64, 581: 7Sam
Davies R.L., Birkinshaw M., 1988, ApJS 68, 409
de Vaucouleurs G., et al., 1991, Third Reference Catalogue of Bright Galaxies. Springer–Verlag: RC3
Fairall A.P., Jones A., 1991, Pub. Dept. of Astron., Univ. Cape Town, N.11, South Africa
Franx M., Illingworth G.D., Heckman T., 1989, ApJ 344, 613
Galletta G., 1996, in Barred Galaxies IAU Coll. No. 157, ASP Conf. Ser. No. 91, Buta R., Crocker D.A., Elmegreen B.G. (eds.) p. 429
Gonzalez J.J., 1993, PhD Thesis, University of California, Santa Cruz: G93.
Hau G.K.T., Thomson R.C., 1994, MNRAS 270, L23
Hechman T.M., 1980, A&A 87, 142
Heyl J.S., Hernquist L., Spergel D.N., 1996, ApJ 463, 69
Ho L.C., 1996, in Physics of lines, Koratckar et al. (eds.) ASPC (in press)
Jedrzejewski R.I., Schechter P.L., 1989, AJ 98, 147
Karachentsev, I.D., 1972, Catalogue of Isolated Pairs of Galaxies in the Northern Hemisphere, Soobshch. Spets. Astrophiz. Obs. 7, 3
Lauberts A., Valentijn E.A., 1989, The Surface Photometry Catalogue of the ESO–Uppsala Galaxies, ESO: ESO-LV.
Longhetti M., Rampazzo R., Bressan A., Chiosi C., 1997a (submitted) (Paper I)
Longhetti, Bressan A., Chiosi C., Rampazzo R., 1997b (in preparation) (Paper III)
Malin D.F., Carter D., 1983, ApJ 274, 534
Plana H., Boulesteix J., 1996, A&A 307, 391
Phillips M.M., Jenkins C.R., Dopita M.A., Sadler E.M., Binette L., 1986, AJ 91, 1062
Prugniel Ph., Simien F., 1996, A&A 309, 749: PS96
Rampazzo R., 1987, Atti. Ist. Ven. Sc. Lett. Arti, Tomo CXLV, p. 81
Rampazzo R., 1988, A&A 204, 81
Reduzzi L., Rampazzo R., 1995, A. Let. Com. 30, Nos. 1-6, 1: RR95
Reduzzi L., Rampazzo R., 1996, A&A 116, 515: RR96
Schiminovic D., Van Gorkom J.H., Van der Hulst J.M., Malin D.F., 1995, ApJ 444, L77
Schweizer F., 1981, ApJ 246, 722
Simien F., Prugniel Ph., 1997, A&AS (in press)
Thomson R.C., 1991, MNRAS 253, 256
Tully B., 1988, in Nearby Galaxies Catalog. Cambridge Univ. Press
Veilleux S., Osterbrock D.E., 1987, ApJS 63, 295
Whitmore B.C., McElroy D.B., Tonry J.L., 1985, ApJS 59, 1
Whitmore B.C., McElroy D.B., Schweizer F., 1987, ApJ 314, 439